# Modeling, Identification, and Predictive Control of a Driver Steering Assistance System

Ziya Ercan, Ashwin Carvalho, Metin Gokasan, and Francesco Borrelli

***Abstract*—This paper presents the design of a driver steering assistance system, which provides a corrective torque in order to guide the driver. While designing such a system, it is important to consider the interactions since the driver modifies the transfer function from the control input to the output of interest during a shared steering task. The novelty of our approach lies in the formulation of the predictive controller, which employs a model of the driver-in-the-loop steering dynamics, where an online parameter identification scheme is proposed to track the time-varying parameters of the process. An optimal guidance torque is calculated with respect to the level of interaction using the updated model. We validate the proposed approach by performing an experimental study with five participants in a guided lane, keeping task under different interaction behaviors of participants. The results show the system capability to adapt the control input based on the driver's acceptance on the torque intervention.**

***Index Terms*—Haptic guidance systems, human–machine interaction, model predictive control (MPC), motor driven power steering system (MDPS), recursive parameter estimation.**

## I. Introduction

ADVANCED driver assistance systems have been one of the most important research directions for mitigating road accidents in the automotive industry. Advances in sensor, actuator, and computing technologies have helped to commercialize active safety features for assisting the driver in hazardous situations [1].

This paper focuses on driver steering assistance systems (DSAS), which use the steering actuator of the vehicle to modify the lateral dynamics in order to improve safety. We particularly consider the case where there is a direct mechanical coupling between the driver and the steering mechanism such as the motor driven power steering (MDPS) system. In this implementation, both the driver and the assistance system share the same physical interface (i.e., the steering wheel) and apply torque to perform the steering task cooperatively. The assistance system could apply a corrective/guidance torque to the steering column and the driver feels the haptic guidance directly on the steering wheel.

The DSAS that are designed based on haptic shared control could be an important milestone for road safety by providing continuous torque guidance to the driver, hence filling the gap between manual driving and autonomous driving. These type of systems are also referred to as haptic guidance systems [2] and related works have been presented in [3]–[7] for scenarios such as lane keeping/changing and collision avoidance. The use of haptic guidance systems for the shared steering task has been validated to be an effective and beneficial way to support and guide drivers during difficult driving tasks [8].

In [9], it is shown that integrating a driver steering model within the control architecture enhances the performance, as the controller takes the driver's intention into account. In the literature, the steering control behavior of the driver is generally modeled as a preview controller based on the future road trajectory [10]. However, this approach does not consider the interaction dynamics between the steering system and the driver. It has been acknowledged from the previous works in [11], [12], and [2] that integrating the neuromuscular dynamics of the driver is important for the assistance system to account for human–machine interactions in shared control.

The assistance system should also be able to evaluate the control objectives (e.g., assisting the driver with minimum conflict, improving safety). These objectives could be formulated as a performance index in the control structure. For example in [13], the human–machine interaction is formulated as a cooperation criteria in the performance index of the controller. On the other hand, a control authority logic based on a weighting function is presented in [9] to determine the cooperation level to minimize the conflicts. The authors in [14] proposed to tune the parameters of a simple gain controller for each participant to minimize the conflicts. However, it is concluded that a more advanced control strategy and driver model are needed to improve the performance of the haptic guidance system.

In [15], the shared control problem is modeled as a differential game for a known driver model. However, it is not practical to have a perfect driver model because of the inherited uncertainty of the modeling and the time-varying response of the driver to the intervention. Saleh *et al.* in [13] provided a robustness analysis of the controller with respect to the uncertainties in the driver model without considering the driver's response to the guidance torque. An online method to estimate the mechanical impedance properties of driver's arm during steering maneuvers

Manuscript received June 24, 2016; revised November 9, 2016, January 16, 2017, and March 29, 2017; accepted May 29, 2017. The work of Z. Ercan was supported by a scholarship provided by the Scientific and Technological Research Council of Turkey between 2015 and 2016. This paper was recommended by Associate Editor R. Toledo. *(Corresponding author: Ziya Ercan.)*

Z. Ercan and M. Gokasan are with the Department of Control and Automation Engineering, Istanbul Technical University, Istanbul 34467, Turkey (e-mail: zyercan@gmail.com; gokasan@itu.edu.tr).

A. Carvalho and F. Borrelli are with the Department of Mechanical Engineering, University of California, Berkeley, Berkeley, CA 94720 USA (e-mail: ashwinmark05@gmail.com; fborrelli@me.berkeley.edu).

Color versions of one or more of the figures in this paper are available online at http://ieeexplore.ieee.org.

Digital Object Identifier 10.1109/THMS.2017.2717881

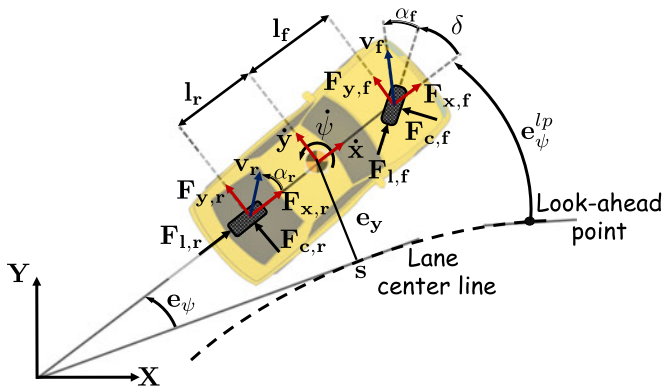


Fig. 1. Notation used in the bicycle model.

is presented in [16]. However, the interaction dynamics between the driver and the guidance torque is not covered.

This paper has two contributions. First, we focus on modeling the interaction dynamics between the driver and the assistance system for a vehicle equipped with an MDPS system. We performed experiments by commanding an open-loop torque input to the MDPS actuator while the driver is holding the steering wheel with different levels of interaction. The results show that the driver has a considerable effect on changing the transfer function from the commanded torque input to the steering wheel angle. This time-varying behavior of the driver should be accounted by the controller to enhance the performance of the assistance system. Therefore, we propose to update the parameters of the driver-in-the-loop steering model online by using a recursive identification method.

In the second part, we use a model predictive control (MPC) for the controller of the assistance system, where the performance objective includes the trajectory tracking and minimum control effort. We conducted an experimental study with five participants to test the performance of the proposed assistance system. While most of the presented work in the literature [2], [13], [17] is implemented by using a driving simulator, in this paper we performed experiments by using a test vehicle with an MDPS system.

This paper is organized as follows. We introduce the models for vehicle dynamics and the steering system in Sections II and III, respectively. The driver-in-the-loop steering model is formulated in Section IV. We propose to use a recursive least squares (RLS) method to identify the parameters of the driver-in-the-loop steering model and present the experimental results in Section V. The paper progresses with presenting the MPC framework used in the proposed assistance system and discussing the experimental study results in Sections VI and VII, respectively. Finally, Section VIII concludes the paper and outlines the future work.

## II. Vehicle Model

We use a bicycle model to describe the dynamics of the ego vehicle (i.e., where the controller action is implemented), as illustrated in Fig. 1. The equations given in (1a)–(1c) are defined in vehicle body frame and the equations given in (1d)–(1f) describe the motion of the vehicle in a road-aligned coordinate frame [18]

$$m\ddot{x} = m\dot{\psi}\dot{y} + 2(F_{x,f} + F_{x,r}) - F_{\text{ext}} \tag{1a}$$

$$m\ddot{y} = -m\dot{\psi}\dot{x} + 2(F_{y,f} + F_{y,r}) \tag{1b}$$

$$I_z\ddot{\psi} = 2(l_f F_{y,f} - l_r F_{y,r}) \tag{1c}$$

$$\dot{e}_\psi = \dot{\psi} - \kappa\dot{s} \tag{1d}$$

$$\dot{e}_y = \dot{x}\sin(e_\psi) + \dot{y}\cos(e_\psi) \tag{1e}$$

$$\dot{s} = \frac{1}{1-\kappa e_y}\Big(\dot{x}\cos(e_\psi) - \dot{y}\sin(e_\psi)\Big). \tag{1f}$$

The longitudinal and lateral velocity of the center of gravity (CoG) are denoted as $\dot{x}$ and $\dot{y}$. The yaw rate $\dot{\psi}$ denotes the rotation of CoG around $z$-axis. The states $e_y$ and $e_\psi$ denote the lateral position of the vehicle with respect to the lane center line and the orientation of the vehicle with respect to the tangent at the lane center line. The longitudinal position of the vehicle along lane center line is denoted as $s$. The parameters of the vehicle model are mass $m$, moment of inertia $I_z$, and distances from the CoG to front and rear axles, denoted as $l_f$ and $l_r$, respectively. The curvature of the road is denoted by $\kappa$ and $e_\psi^{lp}$ denotes the orientation error with respect to a look-ahead point.

*Remark 1:* We assume that a vision system provides estimations of $\kappa$ and $e_\psi^{lp}$ for a finite time horizon.

We consider a front steerable vehicle (i.e., $\delta_f = \delta$, $\delta_r = 0$), where $\delta_f$ and $\delta_r$ denote the road steering angle of the front tires and rear tires, respectively. We assume a linear steering gear ratio $N_s$ with $\theta_s = N_s\delta$, where $\theta_s$ is the steering (hand) wheel angle.

The vehicle is assumed to be operating in the linear region of lateral tire forces (i.e., small tire slip angles), where the front (rear) lateral tire force $F_{c,f}$ ($F_{c,r}$) is proportional to the front (rear) tire slip angle $\alpha_f$ ($\alpha_r$). That is

$$F_{c,i} = -C_{\alpha_i}\alpha_i, \qquad i \in \{f, r\} \tag{2}$$

where $C_{\alpha_f}$ and $C_{\alpha_r}$ denote the cornering stiffnesses of the front and rear tires, respectively. The numerical values of the cornering stiffnesses are identified from experimental data using a standard parameter identification method as presented in [19]. The slip angles $\alpha_f$ and $\alpha_r$ are approximated as

$$\alpha_f = \frac{\dot{y} + l_f\dot{\psi}}{\dot{x}} - \delta, \quad \alpha_r = \frac{\dot{y} - l_r\dot{\psi}}{\dot{x}}. \tag{3}$$

The tire forces acting on the CoG in the vehicle body frame are represented by a rotational transformation as

$$F_{y,i} = F_{l,i}\sin(\delta_i) + F_{c,i}\cos(\delta_i) \tag{4a}$$

$$F_{x,i} = F_{l,i}\cos(\delta_i) - F_{c,i}\sin(\delta_i), \quad i \in \{f, r\}. \tag{4b}$$

In this paper, we focus on the lateral control of the vehicle, therefore we assume the net longitudinal force acting on the vehicle dynamics is zero. We assume that either a speed controller or the driver tracks the desired longitudinal speed and generates required longitudinal tire force components (i.e., $F_{l,f}$ and $F_{l,r}$) to compensate both for the external forces $F_{\text{ext}}$ such as

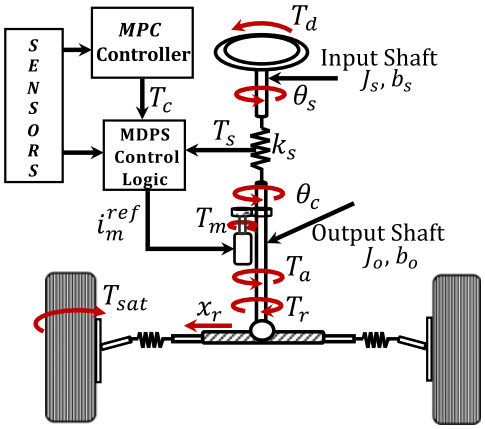


Fig. 2. Steering mechanism of a vehicle equipped with MDPS system. The predictive controller of the proposed DSAS is implemented in the block "MPC Controller."

aerodynamic drag force and the force due to rolling resistance and also for the centripetal acceleration component $\dot{\psi}\dot{y}$.

*Remark 2:* It is possible to extend the proposed framework by including a longitudinal tire model for $F_{l,f}$ and $F_{l,r}$ to account for the longitudinal control behavior of the driver in the vehicle model presented in (1).

In order to include the human–machine interactions, which takes place in the steering (hand) wheel, we need a model that describes the rotational dynamics of the steering mechanism, where the driver and controller both exert torques. This is discussed in Section III.

## III. Modeling the Steering Mechanism of the Vehicle

We consider a column type MDPS system, which consists of a hand wheel and a steering column, a torque sensor (a torsion bar and electronics), an electric motor and control unit, a reduction gear and a rack and pinion mechanism. The steering system of the vehicle is illustrated in Fig. 2.

The MDPS system works as follows. When the driver applies torque $T_d$ on the hand wheel, the torque sensor measures the column torque $T_s$, which indicates the steering request of the driver. During a regular operation, MDPS control logic calculates a torque assistance $\bar{T}_a$, which reduces the steering effort of the driver while enhancing the steering (road) feel by compensating undesired dynamics. On the other hand, the MDPS control logic can also superimpose a torque overlay $T_c$ to $\bar{T}_a$, which enables the implementation of additional safety and comfort features such as lane keeping assist. The functionality of MDPS is preserved for driver's convenience since the basic assist functions are not disabled while using the torque overlay function [20].

The motor torque reference is calculated as $T_m^{\text{ref}} = (\bar{T}_a + T_c)/N_m$ by the MDPS control logic. This is converted to the motor current reference by $i_m^{\text{ref}} = k_t^{-1} T_m^{\text{ref}}$, where $k_t$ is the torque constant. Finally, the required pulse width modulation signals are generated to achieve the desired motor torque $T_m$ and the assist torque $T_a = N_m T_m$ is applied to the steering column through a reduction gear with a gear ratio of $N_m$.

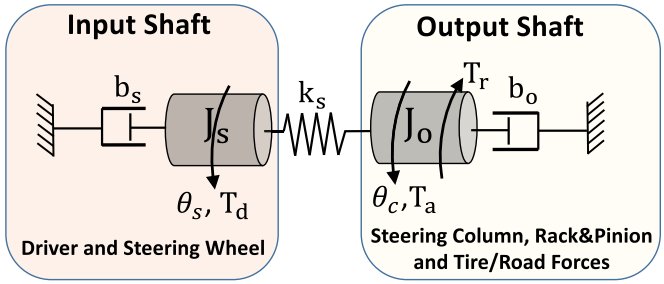


Fig. 3. Free-body diagram of the steering mechanism. The system is separated into two lumped inertia models because of the existence of a stiff torsion bar which couples the input and output shaft dynamics.

A simplified free-body diagram of the steering system is illustrated in Fig. 3 and it is represented by two lumped inertia models separated by a torsion bar with stiffness coefficient $k_s$ (see $k_s$ in Fig. 2). The driver exerts torque ($T_d$) to the hand wheel modeled by inertia $J_s$ and viscous damping $b_s$.

The linearized equation of motion of the input shaft dynamics is described as

$$J_s\ddot{\theta}_s = -b_s\dot{\theta}_s - T_s + T_d \tag{5}$$

where $T_s = k_s(\theta_s - \theta_c)$ and $\theta_c$ is the steering column angle.

The linearized equation of motion of the output shaft dynamics is described as

$$J_o\ddot{\theta}_c = -b_o\dot{\theta}_c + T_s + T_a - T_r \tag{6}$$

where $J_o$ and $b_o$ are the equivalent inertia and damping of the output shaft. The assist torque $T_a$, which is defined previously, and the road reaction torque $T_r = F_r r_p$ act on the output shaft inertia. The road reaction force acting on the rack is denoted by $F_r$ and the radius of the pinion is denoted by $r_p$. Assuming small caster and camber angles, these variables are simply calculated by

$$lF_r = \frac{T_{\text{sat}}}{l_n}, \quad T_{\text{sat}} = t_p F_{c,f} \tag{7}$$

where $T_{\text{sat}}$ is the self-aligning torque generated in the front tires, $t_p$ is the pneumatic trail, and $l_n$ is the length of the knuckle arm [21].

Equations (5) and (6) describe a two degree-of-freedom rotational dynamics (i.e., $\theta_s$ and $\theta_c$) including the assist torque $T_a$, which is calculated by a complicated control framework (i.e., MDPS control logic in Fig. 2) [22]. In this paper, we do not consider the control design for calculating the assist torque since we cannot modify (overwrite) the MDPS control logic of the test vehicle. Therefore, we focused on the input shaft dynamics in (5), where the human–machine interactions take place rather than the output shaft dynamics. We assume that the assist torque $T_a$ in (6) controls the output shaft dynamics such that the driver receives torque feedback $T_r^d$ from the road (steering feel) in regular MDPS operation (i.e., $T_c = 0$). Therefore when the driver grips the hand wheel, we assume that $T_s = T_r^d$ and it is simply modeled as

$$T_r^d = b_r(t)\dot{\theta}_s + k_r(t)\theta_s \tag{8}$$

where the values of $k_r(t)$ and $b_r(t)$ could be changed to adjust the steering feel of the driver [23].

On the other hand, the steering feel of the driver could be modified by using the torque overlay function and we assume that the steering column torque under MDPS overlay torque $T_c$ is described by

$$T_s = T_r^d - T_c. \tag{9}$$

Finally, we can rewrite (5) by using (9) as

$$J_s\ddot{\theta}_s = -b_s\dot{\theta}_s - (T_r^d - T_c) + T_d \tag{10}$$

where the driver-in-the-loop steering model will be derived using (10) in Section IV.

## IV. Modeling the Driver Torque

In this section, we model the driver torque $T_d$ as a sum of two components, where the first component $T_{d,s}$ corresponds to the torque effort of the driver for steering the vehicle and the second component $T_{d,r}$ corresponds to the torque generated by the driver's arms in order to restrict the controller's action $T_c$ while holding the steering wheel (i.e., $T_d = T_{d,s} + T_{d,r}$). Both of the components $T_{d,s}$ and $T_{d,r}$ will be discussed next.

### A. Steering Torque Model of the Driver

The steering torque of the driver could be considered as the sum of feedback (FB) and feedforward (FF) compensations [24]. The FB term represents the torque to track a desired steering wheel angle $\theta_s^d$ and the FF term compensates for the effective road reaction torque on the hand wheel $T_r^d$. The resulting model is defined as

$$T_{d,s} = -K_{ds}(\theta_s - \theta_s^d) + T_r^d \tag{11}$$

where $\theta_s^d$ can be calculated by using a preview driver model, which represents the driver's steering behavior as a linear function of lateral position $e_y$ and orientation error $e_\psi^{lp}$ with respect to a look-ahead point, as given in Fig. 1. The coefficient of the preview model given in (12) could be estimated using a nonlinear least squares approach from driving data [25].

$$\theta_s^d = K_2 e_y + K_3 e_\psi^{lp}. \tag{12}$$

### B. Impedance Model of the Driver's Arms

Previous studies show that the mechanical impedance of the driver's arms while holding the steering wheel could be represented by a linear "mass-damper-spring" model [2], [17]. The drivers can adapt their mechanical impedance properties by activating the arm muscles when there is a conflict in objectives of the driver and the assistance system. Therefore, it is essential to account for these interactions in the control design. We model the mechanical impedance of the driver's arms as

$$-T_{d,r} = J_d(t)\ddot{\theta}_s + b_d(t)\dot{\theta}_s + k_d(t)\theta_s \tag{13}$$

where $J_d$, $b_d$, and $k_d$ represent the equivalent inertia, damping, and stiffness properties of the impedance model of the driver's arms as seen at the steering wheel axis. These time-varying parameters include the passive arm (i.e., relaxed muscles) and the cocontracted state (i.e., increased damping and stiffness) impedance properties of the arms.

As the driver holds the hand wheel, the mechanical impedance properties of the driver and the steering system are integrated as one lumped inertia model. We can compactly describe the equation of motion for the driver-in-the-loop steering model by using the equations in (10), (11), and (13) as

$$J_{\text{eq}}(t)\ddot{\theta}_s = -b_{eq}(t)\dot{\theta}_s - k_{\text{eq}}(t)\theta_s + T_c + T_{d,s} \tag{14}$$

where $J_{\text{eq}}(t) = J_s + J_d(t)$, $b_{\text{eq}}(t) = b_s + b_d(t) + b_r(t)$, and $k_{\text{eq}}(t) = k_d(t) + k_r(t)$ describe the equivalent inertia, damping, and stiffness of the driver-in-the-loop steering model. We define the hand wheel rate as $\omega_s = \dot{\theta}_s$. The state-space representation of the driver-in-the-loop steering model is given as

$$\frac{d}{dt}\begin{bmatrix}\theta_s \\ \omega_s\end{bmatrix} = \begin{bmatrix}0 & 1 \\ -\frac{k_{\text{eq}}(t)}{J_{\text{eq}}(t)} & -\frac{b_{\text{eq}}(t)}{J_{\text{eq}}(t)}\end{bmatrix}\begin{bmatrix}\theta_s \\ \omega_s\end{bmatrix} + \begin{bmatrix}0 \\ \frac{1}{J_{\text{eq}}(t)}\end{bmatrix}(T_c + T_{d,s}). \tag{15}$$

We approximate the continuous-time model of the process given in (15) by using a forward difference method. For the sake of clarity, we drop the subscript and let $\theta = \theta_s$ and $\omega = \omega_s$. The discrete-time model of the process is obtained as

$$\begin{bmatrix}\theta_{k+1} \\ \omega_{k+1}\end{bmatrix} = \begin{bmatrix}1 & \Delta t \\ \varphi_{1,k} & \varphi_{2,k}\end{bmatrix}\begin{bmatrix}\theta_k \\ \omega_k\end{bmatrix} + \begin{bmatrix}0 \\ \varphi_{3,k}\end{bmatrix}(u_k + d_k) \tag{16}$$

where the time-varying discrete-time parameters are defined as $\varphi_{1,k} = -\frac{\Delta t k_{\text{eq}}(t)}{J_{\text{eq}}(t)}$, $\varphi_{2,k} = 1 - \frac{\Delta t b_{\text{eq}}(t)}{J_{\text{eq}}(t)}$, and $\varphi_{3,k} = \frac{\Delta t}{J_{\text{eq}}(t)}$. The control input is denoted as $u_k = T_c$ and the driver torque input is denoted as $d_k = T_{d,s}$, which is a function of vehicle states and road preview.

We discretize the set of differential equations given in (1) using a forward difference method and augment the resulting discrete-time steering model presented in (16). The augmented prediction model, which is employed in the controller, can be compactly written as

$$\zeta_{k+1} = f^d(\zeta_k, u_k, \kappa_k) \tag{17}$$

where the state vector is $\zeta = [\dot{x}, \dot{y}, \dot{\psi}, e_\psi, e_y, s, \theta, \omega]^\intercal$, the control input is the overlay torque $u = T_c$, and $\kappa$ is the estimate of the curvature. $k$ denotes the current discrete-time step and $\Delta t$ is the sampling period such that $t = k\Delta t$.

## V. Parameter Identification of Driver-in-the-loop Steering Model

The objective of this section is to describe the identification method of the mechanical impedance properties of the driver-in-the-loop steering model (i.e., $J_{eq}$, $b_{eq}$, $k_{eq}$) in (14) online, since they vary as the driver interacts with the guidance torque. In order to account for these changes, it is important to update the parameters recursively in real-time while the controller is operating.

*Remark 3:* There are human factor studies in the literature about the identification of the mechanical impedance properties of the driver's arms while holding the hand wheel with respect to the open-loop input signal (i.e., torque disturbance) in [2], [17].

The focus of this section is to validate the proposed recursive identification method experimentally.

### A. Experimental Procedure

We consider the following three cases to identify the mechanical impedance properties of the driver-in-the-loop steering model, where the overlay torque (control) input is the source of motion.

*Case 1—Hands Off*: The aim of this case is to identify the response of the steering system to the control input $T_c$ in order to model the steering dynamics for autonomous driving purposes (i.e., $T_d = 0$).

*Case 2—Compliant Driver*: We ask the driver to hold the hand wheel, without actively steering (i.e., $T_{d,s} = 0$), and let the control input $T_c$ to steer the vehicle.

*Case 3—Stiff Driver:* The driver holds the hand wheel firmly and resists the motion by increasing the impedance through muscle activation without actively steering (i.e., $T_{d,s} = 0$).

### B. Identification Method

We use an RLS identification method for tracking the time-varying parameters of the system presented in (15). The exponential forgetting and resetting algorithm is chosen for its good convergence and tracking performance under poor excitation of the dynamics. This method incorporates both exponential data forgetting and covariance resetting [26].

We propose the following linear regression model $\hat{y}_k = X_k \hat{\Phi}_{k-1}^{\intercal}$, which is derived from the discrete-time steering dynamics of (16), where $\hat{y}_k$ is the model output at time step $k$, $X_k = [1,\ \theta_{k-1},\ \omega_{k-1},\ T_{c,k-1}]$ is the regression vector and the estimated parameters are $\hat{\Phi}_{k-1} = [\hat{\varphi}_{0,k-1}, \ldots, \hat{\varphi}_{3,k-1}]$.

*Remark 4:* We add a bias term $\hat{\varphi}_{0,k-1}$ in the regression model to account for unmodeled input disturbances.

The calculation steps of EFRA are expressed as follows. The algorithm starts from an initial value of the covariance matrix (e.g., $P_0 = \sigma I, \sigma \gg 0$) and parameter vector (e.g., $\hat{\Phi}_0 = \mathbf{0}$). At each time step, the model output $\hat{y}_k$ and the filter gain $K_k$ is calculated in (18) and (19). When a new measurement $y_k = \omega_k$ is acquired, the parameter vector $\hat{\Phi}_k$ is updated in (20) and finally the covariance matrix $P_k$ is updated by using (21). The parameters $\lambda$ is the forgetting factor, $\alpha$ is the filter gain. Both $\beta$ and $\gamma$ are used for covariance resetting and normalization. The parameters are selected as $\alpha = 0.5, \lambda = 0.98$, and $\beta = \gamma = 0.005$.

$$\hat{y}_k = X_k \hat{\Phi}_{k-1}^{\intercal} \tag{18}$$

$$K_k = \frac{\alpha P_{k-1} X_k}{\alpha + X_k^{\intercal} P_{k-1} X_k} \tag{19}$$

$$\hat{\Phi}_k = \hat{\Phi}_{k-1} + K_k (y_k - \hat{y}_k) \tag{20}$$

$$P_k = \frac{1}{\lambda}(I - K_k X_k^{\intercal}) + \beta I - \gamma P_{k-1}^2. \tag{21}$$

### C. Results and Discussion

We performed experiments with a test vehicle equipped with MDPS system while traveling at a constant longitudinal speed of 15 m/s in Hyundai–Kia California Proving Grounds. We commanded an overlay torque sine sweep reference, $T_c(t) = 3\sin(2\pi f_c t)$ N·m, where $f_c = [0.2, 0.8]$ Hz, to MDPS control logic at the sampling frequency $f_s = 100$ Hz. The driver-in-the-loop steering model parameters were identified recursively at 10 Hz using the algorithm discussed in previous section, while the steering system was excited by the control input $T_c$.

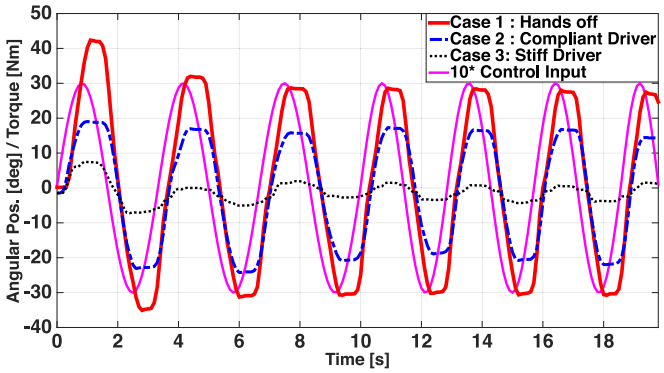


Fig. 4. Hand wheel angle $\theta$ response to the overlay torque input $T_c$ for the test cases presented in Section V-A.

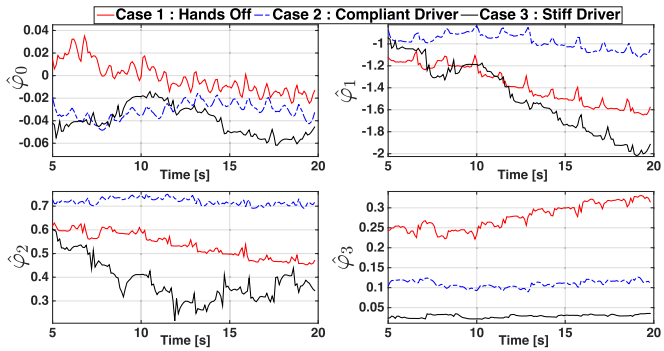


Fig. 5. Estimated parameters of the driver-in-the-loop steering model presented in (16).

The hand wheel angle measurements of all the test cases of a random trial, performed by a participant, are illustrated in Fig. 4 along with the commanded overlay torque input. The estimated parameters of the regression model is illustrated in Fig. 5. It is clear that $\hat{\varphi}_3$ has the highest value for Case 1 among the other cases since it has the least impedance. The total impedance of the system increases as the driver cocontracts the muscles and resists the overlay torque (i.e., tensed condition). It is observed that overlay torque coefficient (i.e., $\hat{\varphi}_3$) decreases as the impedance of the system increases.

We also illustrate the estimated mechanical impedance properties of the driver-in-the-loop model (14) that is converted from the identified parameters in Fig. 6. As expected, there is a significant increase in damping and stiffness of the system as the driver cocontracts the muscles to generate reaction torque. We present the average values of the mechanical impedance properties of five trials with the same participant in Table I.

*Remark 5:* When the excitation of the steering dynamics is poor (i.e., when there is no motion in the hand wheel or the overlay torque input excitation is zero), the estimated

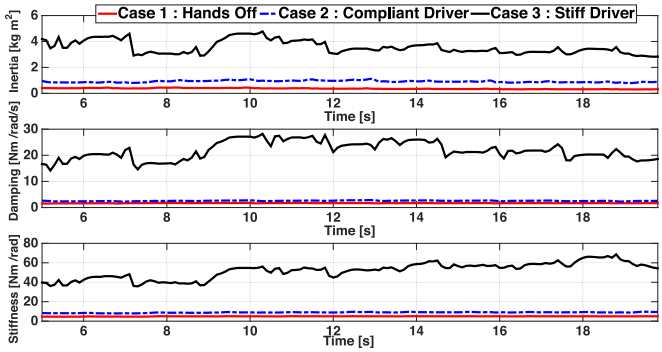


Fig. 6. Estimated mechanical impedance properties ($J_{eq}$, $b_{eq}$, $k_{eq}$) of the driver-in-the-loop steering model presented in (15).

TABLE I
AVERAGE VALUES OF THE MECHANICAL IMPEDANCE PROPERTIES

| Case | Inertia [kg·m$^2$] | Damping [N·m/rad/s] | Stiffness [N·m/rad] |
|---|---|---|---|
| Case 1 | 0.32 | 1.63 | 4.98 |
| Case 2 | 0.84 | 2.52 | 9.40 |
| Case 3 | 3.90 | 19.0 | 53.33 |

discrete-time parameters might fail to converge to their correct values. Therefore, the calculation of the mechanical impedance properties (i.e., $J_{eq}(t)$, $b_{eq}(t)$, $k_{eq}(t)$) from estimated discrete-time model parameters (i.e., $\hat{\varphi}_i,\ i = 0, \ldots, 3$) might result in unreliable values.

## VI. Model Predictive Controller Design

In this section, we present the design of the controller, which employs the prediction model presented in (17). The safety and input constraints for the controller are discussed in Sections VI-A and VI-B, respectively, followed by the optimization problem formulation in Section VI-C.

### A. Safety Constraints

The most important objective of the proposed system is to keep the vehicle in the drivable part of the road therefore improving safety. This is achieved by imposing upper and lower bounds on the lateral position $e_y$ of the ego vehicle as

$$e_{y_{\min}} \leq e_y \leq e_{y_{\max}} \tag{22}$$

where the bounds are determined by the lane width $w_{\text{lane}}$, vehicle width $w_c$, and a safety margin $d_{\text{safe}}$.

*Remark 6:* The general collision avoidance constraints in highway driving scenarios could be formulated as in [27]. We do not include the formulation since it is not the main focus of this paper.

### B. Input Constraints

We enforce the following magnitude and the rate constraints on the overlay torque (i.e., actuator input) $T_c$ in order to have a smooth and adequate level of torque guidance considering the comfort of the driver

$$T_{\min} \leq T_c \leq T_{\max} \tag{23a}$$

$$\Delta T_{\min} \leq \Delta T_c \leq \Delta T_{\max}. \tag{23b}$$

### C. MPC Formulation

The constrained finite time optimal control problem given in (24) is solved at each sampling interval $\Delta t_c$. The first element of the optimal input sequence is applied to the steering actuator and this process is repeated at the next time step using the state measurements as the initial condition. The optimization variables are the MDPS overlay torque (i.e., $u = T_c$) and the slack variable $\epsilon$

$$\min_{\mathbf{u}_k, \epsilon} \sum_{i=0}^{N-1} (\|u_{i|k}\|_Q^2 + \|\Delta u_{i|k}\|_R^2) + \sum_{i=1}^{N} \|\zeta_{i|k} - \zeta_{i|k}^r\|_W^2 + M\epsilon \tag{24a}$$

$$\text{s.t. } \zeta_{i+1|k} = f_d(\zeta_{i|k}, u_{i|k}, \kappa_{i|k}) \tag{24b}$$

$$T_{\min} \leq u_{i|k} \leq T_{\max} \tag{24c}$$

$$\Delta T_{\min} \leq \Delta u_{i|k} \leq \Delta T_{\max} \tag{24d}$$

$$e_{y_{\min}} - \epsilon \leq e_{y_{i+1|k}} \leq e_{y_{\max}} + \epsilon, \quad \epsilon \geq 0 \quad (i = 0, \ldots, N-1) \tag{24e}$$

$$\zeta_{0|k} = \zeta_k, \quad u_{-1|k} = u_{k-1} \tag{24f}$$

where $N$ is the prediction horizon and $\|z\|_Z^2 = z^T Z z$. $\zeta_{i|k}$ denotes the $i$th state prediction at time step $k$ obtained by applying the optimal input sequence $\mathbf{u}_k = \{u_{0|k}, u_{1|k}, \ldots, u_{N-1|k}\}$ to the discrete-time dynamics (24b) starting from the measured state at the current time step (24f). The sampling interval for discretization of the continuous-time dynamics is $\Delta t_{\text{mpc}}$.

We impose the safety constraints (22) as soft constraints (24e) by introducing the slack variable $\epsilon$ in order to keep the optimization problem feasible in any case of possible constraint violations due to model mismatch. The cost function in (24a) reflects the control objectives in shared driving tasks. We penalize the magnitude and rate of the control input using the corresponding weights $Q$ and $R$ in order to utilize smooth and minimal control action. The state tracking term in (24a) enforces the controller to track desired state trajectory $\zeta^r$ using the weight matrix $W$. We penalize the states $e_y$, $\dot{y}$, and $\dot{\psi}$ to achieve a smooth trajectory tracking performance. In this paper, the state reference values are given as zero since the objective is lane keeping in a straight road. $M$ is a large number, which penalizes the constraint violation $\epsilon$.

## VII. Experimental Study : Human–Machine Interactions in Lane Keeping Guidance

In this section, we present the results of our experimental study, where the assistance system guides the driver to the lane center line from an initial lateral position while the driver shows different levels of interaction ranging from following the

TABLE II
MPC VEHICLE MODEL PARAMETERS

| Parameter | Value | Parameter | Value |
|---|---|---|---|
| $m$ | 1830 kg | $I_z$ | 3477 kg·m$^2$ |
| $l_f$ | 1.152 m | $l_r$ | 1.693 m |
| $C_{\alpha_f}$ | 40 703 N/rad | $C_{\alpha_r}$ | 64 495 N/rad |
| $w_c$ | 1.86 m | $N_s$ | 14.5 |

TABLE III
MPC DESIGN PARAMETERS

| Parameter | Value | Parameter | Value |
|---|---|---|---|
| $\Delta t_c$ | 0.1 s | $\Delta t_{\text{mpc}}$ | 0.2 s |
| $T_{\min}$ | $-5$ N·m | $\Delta T_{\min}$ | $-10$ N·m/s |
| $T_{\max}$ | 5 N·m | $\Delta T_{\max}$ | 10 N·m/s |
| $e_{y_{\min}}$ | $-0.67$ m | $e_{y_{\max}}$ | 4.07 m |
| $w_{\text{lane}}$ | 3.4 m | $Q, R, M$ | $(15, 10, 1000)$ |
| $W$ | $\mathbf{diag}(0, 5, 5, 0$ $10, 0, 0, 0)$ | $N$ | 12 |
| | | $d_{\text{safe}}$ | 0.1 m |

guidance torque $T_c$ (i.e., compliant driver) to actively resisting it (i.e., stiff driver).

The objective of this study is to show that the proposed approach can identify the corresponding differences in the drivers' mechanical impedance properties and suitably adapt the guidance torque by updating the model employed in the controller with respect to the interaction level.

### A. Experimental Setup

We validate the performance of the proposed DSAS on our test vehicle. Computations are performed on a dSPACE MicroAutoBox II embedded computer running at 900 MHz. Besides the built-in sensors of the vehicle, a forward-looking camera measures the lane boundaries, the curvature of road and the heading of the vehicle with respect to the lane. The steering actuator is a production level MDPS with a torque overlay function for automated driving applications. This allows us to directly request the guidance torque $T_c$ from the MDPS controller. The sensors, embedded computer, and actuators communicate through a controller area network (CAN) bus. The online optimization problem is solved using the general purpose nonlinear solver NPSOL [28]. The parameters used in the vehicle model and in the predictive controller are listed in Tables II and III, respectively.

### B. Experimental Procedure

We performed an experimental study with five participants aged between 25 to 30 years at the Berkeley Global Campus. The vehicle was initially at rest on a straight road (e.g., two lanes in each direction) and was positioned around 1.5 m to the left of the rightmost lane center line. We asked each participant to accelerate and maintain a constant speed of 11 m/s and to check the speed display of the vehicle frequently to simulate a visual distraction. The participants activated the assistance system by pushing a marked button on the hand wheel after passing a visual marking on the road. When the assistance system applied guidance torque to bring the vehicle to the lane center line, we asked the participants to show different neuromuscular response to the guidance torque with respect to the cases presented in Section V-A. In the compliant and stiff driver cases, we asked the participants not to steer actively (i.e., $T_{d,s} = 0$) but to exhibit an impedance-like behavior. We modified the stiff driver case such that we asked the participants to oppose the guidance torque initially and take the hands off the steering wheel after five seconds. Moreover in *Driver Only* case, we asked the participants to perform the lane centering maneuver while the controller was deactivated after passing the same visual marking on the road.

The recursive identification algorithm was also started when the participant activated the controller. The parameters were initialized as $\hat{\Phi}_0 = [0,\ 0,\ 0,\ 0.2]^\intercal$ to introduce a modeling uncertainty to the controller (i.e., the driver-in-the-loop steering model is initially unknown).

### C. Results

We present the results of the test cases that are performed by all participants in Fig. 7. In the *driver only* case, it is observed that participants' lane centering trajectories without the controller are similar in terms of small overshoot but a steady-state error around 0.2 m when they complete the maneuver. Each participant also performed the *hands off* case without holding the hand wheel. There are some differences in the associated plots, which are caused by the different longitudinal speed behavior of the participants. Nevertheless, the controller performance was consistent. We observed an overshoot around 0.25 m and a slow settling time of around 8 s during the trajectory tracking maneuver. This is attributed to improper tuning of the controller since the focus of the paper is not autonomous driving.

If we consider the *compliant driver* case, we see that the response of the participants to the guidance torque is quite different. The spread of the lateral trajectories is significantly larger in the *compliant driver* case than in the *driver only* and *hands off* cases. This result reveals that participants have different levels of interaction with the guidance torque with respect to their individual preferences. Among the five participants, *Participant* 3 and *Participant* 5 exhibited the most extreme responses. *Participant* 3 opposed to the guidance torque more than *Participant* 5 and therefore increased the impedance of the arms because the guidance torque might have felt too aggressive for the participant's preferences. On the other hand, *Participant* 5 followed the guidance torque without introducing a noticeable impedance. The steering system related measurements are also illustrated in Fig. 8. The convex hull of the related measurements shows the steering regions of the different test cases for *Participants* 3 and 5. It is seen that the participants operate in different regions of the measurement space while interacting with the guidance torque of the controller. It is interesting to note that for *Participant* 5, there is a large overlap between the regions corresponding to the *hands off* and *compliant driver* cases. On the other hand, for *Participant* 3, the regions corresponding to

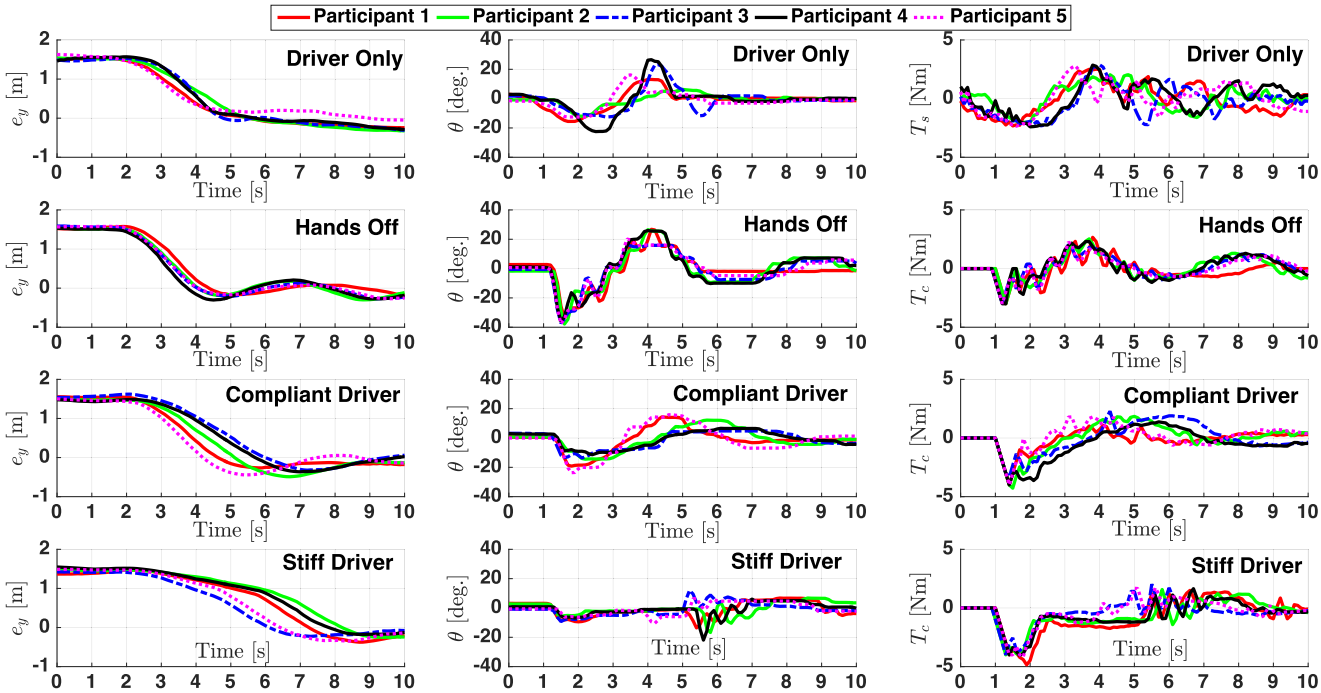


Fig. 7. Comparison of the test cases among five participants. The lateral deviation from lane center line is illustrated in the left columns. The plots in the middle column illustrate the hand wheel angle $\theta$ measurements. Finally, the right top column plot illustrates the steering effort of the participants on the other hand, the rest of the plots illustrate the guidance torque applied by the controller.

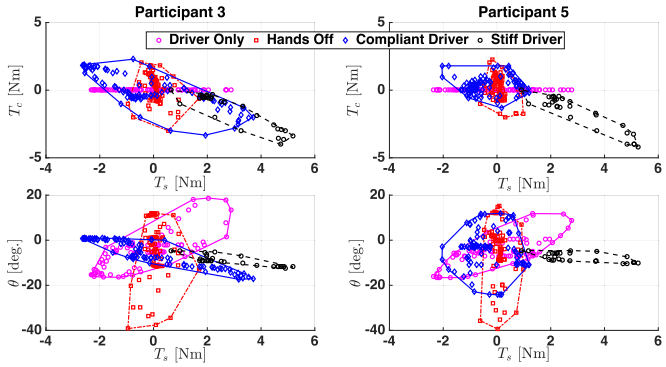


Fig. 8. Plots of the guidance torque ($T_c$) versus the steering column torque ($T_s$) and the hand wheel angle ($\theta$) versus $T_s$ for *Participants* 3 and 5.

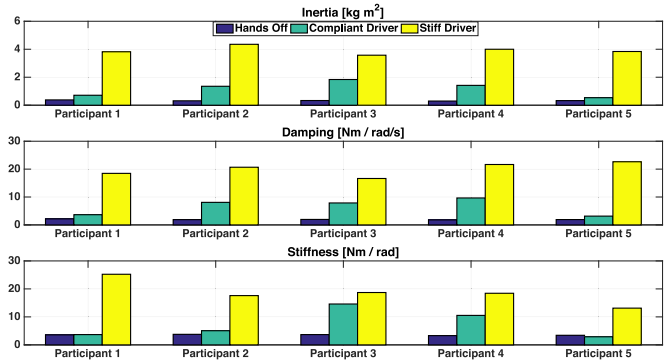


Fig. 9. Mean values of the estimated mechanical impedance properties of the driver-in-the-loop steering model for all participants.

the *compliant driver* and *stiff driver* cases exhibit a relatively large overlap.

In the *stiff driver* case, the participants opposed to the guidance torque by cocontracting their muscles for about 4 s. At $t = 5$ s, the participants released their hands from the steering wheel to introduce an abrupt change in the steering dynamics. The RLS algorithm updated the parameters of the model to account for the changes in the dynamics while the controller applied $T_c$ to track the trajectory. We observed some oscillations in $T_c$ during the transient period of identification before the parameters converged to their steady-state values.

The mean values of mechanical impedance properties are illustrated in Fig. 9. The estimated parameters of the *hands off* case for all participants are similar and close to the values that are presented in Table I. This result validates our assumption that the excitation of the steering system is adequate for the closed-loop identification in the *hands off* case. The average impedance of each participant in the *compliant driver* case varies with respect to how participants responded to the guidance torque. As mentioned earlier, it is observed that *Participants* 2, 3, and 4 introduced more impedance to the steering dynamics than *Participants* 1 and 5. We observed a remarkable increase in the equivalent impedance especially in terms of damping and stiffness during the *stiff driver* case as expected. These results are similar to the values presented in the open-loop identification in Table I.

We investigate the test cases that are performed by *Participant* 1 separately. This participant is chosen randomly with-

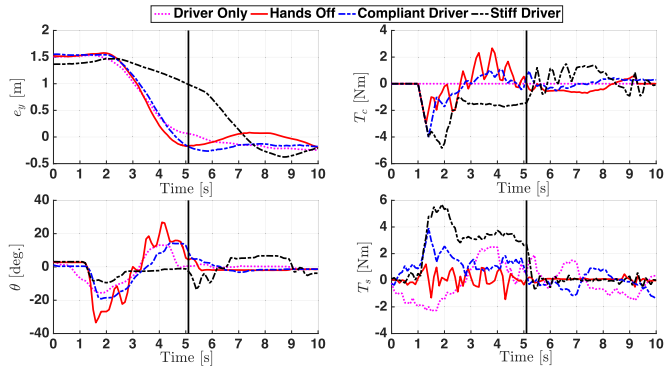


Fig. 10. Individual measurements of test cases that are performed by *Participant* 1. The vertical line is associated with *stiff driver* case and indicates the time when the participant released hands from the steering wheel.

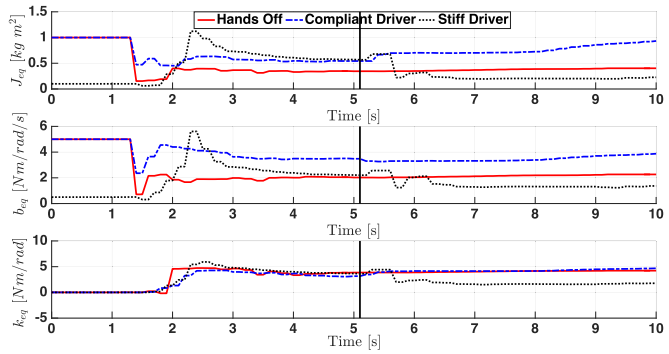


Fig. 11. Estimated mechanical impedance properties of driver-in-the-loop steering model given in (14) for the three test cases. The values of *stiff driver* case is scaled down by a factor of 10. The vertical line is associated with *stiff driver* case and indicates the time when the participant released hands from the steering wheel.

out any bias. The related measurements of the test cases and the estimated impedance properties of the driver-in-the-loop steering model are illustrated in Figs. 10 and 11, respectively. The controller is activated around $t = 1$ s in all test cases except the *driver only* case. If the *stiff driver* case is considered, it is seen that the controller applied a guidance torque around $-4$ N·m after activation. As the participant opposed to the guidance, the RLS algorithm increased the impedance parameters of the steering model employed in the controller. Around $t = 2$ s, the controller started to decrease the guidance torque. This behavior is explained as follows.

The predictive controller calculates the optimal guidance torque that minimizes the objective function. In a lane keeping guidance scenario when there is a conflict between the actions of the driver and the controller, the impedance of the steering model increases. This causes an increase in the input cost since the controller needs a higher amount of corrective torque $T_c$ to steer the vehicle. We would like to stress that when the controller predicts an unsafe situation (e.g., lane/road departure), which corresponds to the violation of constraints, the controller delivers an adequate level of guidance to keep the vehicle in the safe portion of the road even if the driver opposes the intervention. This is caused by the dominant constraint violation penalty in the cost function.

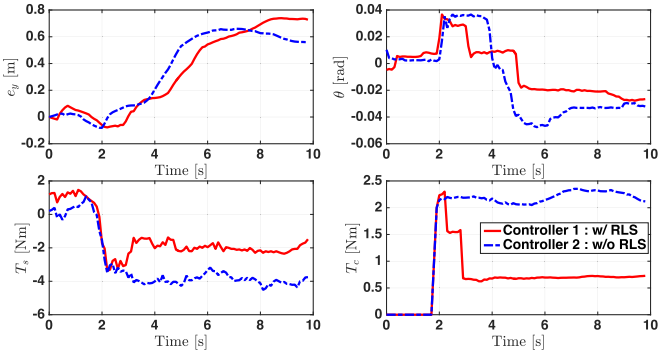


Fig. 12. Results of the experiment with two different controllers.

To introduce an abrupt change in the steering dynamics, the participant released its hands from the steering wheel at $t = 5$ s. However, we observe that the parameters do not converge to the values in the *hands off* case after the participant releases its hands. This is due to the fact that the level of excitation decreases as the vehicle approaches the lane center line. The controller should introduce a sufficient level of excitation to the steering dynamics in order for the parameters to converge to the true values.

### D. Model Comparison

We propose a conflict scenario between the driver and the system during a lane change guidance. In this scenario, the system guides the driver to change the lane but the driver does not agree and opposes the guidance torque to override the system's actions. We present the experimental results of two assistance systems where a recursive parameter identification is employed in *Controller 1* to update the parameters of the driver-in-the-loop steering model and *Controller 2* uses constant parameters (i.e., the average values of Case 2 in Table I), which is illustrated in Fig. 12. In both of the experiments, the driver activated the assistance system around $t = 2$ s and guidance torque is applied to steer the vehicle to the target lane (i.e., $e_y^{\text{ref}} = 3.4$ m). As seen in Fig. 12, *Controller 2* applied the same amount of guidance torque without accounting for driver's interaction behavior therefore increasing the physical workload of the driver. On the other hand, *Controller 1* decreased the guidance torque to a comfortable level hence decreasing the workload of the driver in this conflict situation. The results show the effectiveness of the proposed assistance system to resolve the conflicts in shared steering tasks when the assistance system and the driver have different objectives.

## VIII. Conclusion

In this paper, we present a predictive, driver-in-the-loop control framework for an implementation of a DSAS, which influences the driver by utilizing a guidance torque through the hand wheel. As the system and the driver operate in the same interface, the driver could adapt its neuromuscular response with

respect to the acceptance level. Therefore, we propose to use a recursive identification method to account for the variations in the interaction dynamics. A better control performance is achieved by updating the prediction model in the controller.

We performed an experimental study with five participants to validate the performance. The results show that the assistance system adapts the guidance torque systematically with respect to the interaction level. This approach could be a practical method to resolve conflicts between the driver and the controller while performing a steering task cooperatively. However, it is important to point out that current sample size is a limitation to justify the statistical reliability of the results.

Therefore, as the next step of our research we will conduct an experimental study with a larger sample set in order to assess the generalizability and the reliability of the proposed DSAS. Also, we would like to investigate the system's adaptation to driver's preferences in a long-term driving scenario and show how the driver's experience might affect the assistance system.

## ACKNOWLEDGMENT

The authors would like to thank Dr. S. Lefèvre for interesting discussions and the Hyundai Motor Company for support related to the experiments.

## REFERENCES

[1] S. Sivaraman and M. M. Trivedi, "Towards cooperative, predictive driver assistance," in *Proc. 16th Int. IEEE Conf. Intell. Transp. Syst.*, Oct. 2013, pp. 1719–1724.

[2] D. A. Abbink and M. Mulder, "Neuromuscular analysis as a guideline in designing shared control," *Adv. Haptics*, pp. 499–517, 2010, doi: 10.5772/8696.

[3] P. Griffiths and R. B. Gillespie, "Shared control between human and machine: haptic display of automation during manual control of vehicle heading," in *Proc. 12th Int. Symp. Haptic Interfaces Virtual Environ. Teleoperator Syst.*, Mar. 2004, pp. 358–366.

[4] T. Brandt, T. Sattel, and M. Bohm, "Combining haptic human-machine interaction with predictive path planning for lane-keeping and collision avoidance systems," in *Proc. 2007 IEEE Intell. Vehicles Symp.*, Jun. 2007, pp. 582–587.

[5] K. K. Tsoi, M. Mulder, and D. A. Abbink, "Balancing safety and support: Changing lanes with a haptic lane-keeping support system," in *Proc. IEEE Int. Conf., Syst. Man Cybern.*, Oct. 2010, pp. 1236–1243.

[6] A. Balachandran, M. Brown, S. M. Erlien, and J. C. Gerdes, "Predictive haptic feedback for obstacle avoidance based on model predictive control," *IEEE Trans. Autom. Sci. Eng.*, vol. 13, no. 1, pp. 26–31, Jan. 2016.

[7] K. Iwano, P. Raksincharoensak, and M. Nagai, "A study on shared control between the driver and an active steering control system in emergency obstacle avoidance situations," *IFAC Proc. Vol.*, vol. 47, no. 3, pp. 6338–6343, 2014.

[8] D. A. Abbink, M. Mulder, and E. R. Boer, "Haptic shared control: Smoothly shifting control authority?" *Cognit., Technol. Work*, vol. 14, no. 1, pp. 19–28, 2012.

[9] C. Sentouh, S. Debernard, J. Popieul, and F. Vanderhaegen, "Toward a shared lateral control between driver and steering assist controller," *IFAC Proc. Vol.*, vol. 43, no. 13, pp. 404–409, 2010.

[10] D. J. Cole, A. J. Pick, and A. M. C. Odhams, "Predictive and linear quadratic methods for potential application to modelling driver steering control," *Veh. Syst. Dyn.*, vol. 44, no. 3, pp. 259–284, 2006.

[11] A. J. Pick and D. J. Cole, "A mathematical model of driver steering control including neuromuscular dynamics," *J. Dyn. Syst. Meas. Control*, vol. 130, 2008, Art. no. 031004.

[12] D. J. Cole, "A path-following drivervehicle model with neuromuscular dynamics, including measured and simulated responses to a step in steering angle overlay," *Veh. Syst. Dyn.*, vol. 50, no. 4, pp. 573–596, 2012.

[13] L. Saleh, P. Chevrel, F. Claveau, J.-F. Lafay, and F. Mars, "Shared steering control between a driver and an automation: Stability in the presence of driver behavior uncertainty," *IEEE Trans. Intell. Transp. Syst.*, vol. 14, no. 2, pp. 974–983, Jun. 2013.

[14] R. Boink, M. M. van Paassen, M. Mulder, and D. A. Abbink, "Understanding and reducing conflicts between driver and haptic shared control," in *Proc. 2014 IEEE Int. Conf. Syst., Man, Cybern.*, Oct. 2014, pp. 1510–1515.

[15] M. Flad, J. Otten, S. Schwab, and S. Hohmann, "Steering driver assistance system: A systematic cooperative shared control design approach," in *Proc. 2014 IEEE Int. Conf. Syst., Man, Cybern.*, Oct. 2014, pp. 3585–3592.

[16] A. Marouf, P. Pudlo, C. Sentouh, and M. Djemai, "Identification of human arm viscoelastic properties during vehicle steering maneuver," in *Proc. IEEE Int. Conf., Syst., Man Cybern.*, Oct. 2014, pp. 3342–3347.

[17] A. Pick and D. J. Cole, "Dynamic properties of a driver's arms holding a steering wheel," in *Proc. Inst. Mech. Eng., Part D, J. Automobile Eng.*, vol. 221, no. 12, pp. 1475–1486, 2007.

[18] R. Rajamani, *Vehicle Dynamics and Control* (Mechanical Engineering Series). New York, NY, USA: Springer, 2011.

[19] C. Sierra, E. Tseng, A. Jain, and H. Peng, "Cornering stiffness estimation based on vehicle lateral dynamics," *Veh. Syst. Dyn.*, vol. 44, no. sup1, pp. 24–38, 2006.

[20] W. Kim, Y. S. Son, and C. C. Chung, "Torque overlay-based robust steering wheel angle control of electrical power steering for a lane-keeping system of automated vehicles," *IEEE Trans. Veh. Technol.*, vol. 65, no. 6, pp. 4379–4392, Jun. 2016.

[21] W. Milliken and D. Milliken, *Race Car Vehicle Dynamics* (Premiere Series). vol. 1, Warrendale, PA, USA: SAE, 1995.

[22] A. Marouf, M. Djemai, C. Sentouh, and P. Pudlo, "A new control strategy of an electric-power-assisted steering system," *IEEE Trans. Veh. Technol.*, vol. 61, no. 8, pp. 3574–3589, Oct. 2012.

[23] A. Pick and D. Cole, "Neuromuscular dynamics and the vehicle steering task," *Dyn. Vehicles Roads Tracks*, vol. 41, pp. 182–191, 2003.

[24] S. Zafeiropoulos and S. Di Cairano, "Vehicle yaw dynamics control by torque-based assist systems enforcing driver's steering feel constraints," in *Proc. Amer. Control Conf.*, Jun. 2013, pp. 6746–6751.

[25] A. Gray, M. Ali, Y. Gao, J. K. Hedrick, and F. Borrelli, "A unified approach to threat assessment and control for automotive active safety," *IEEE Trans. Intell. Transp. Syst.*, vol. 14, no. 3, pp. 1490–1499, Sep. 2013.

[26] M. E. Salgado, G. C. Goodwin, and R. H. Middleton, "Modified least squares algorithm incorporating exponential resetting and forgetting," *Int. J. Control*, vol. 47, no. 2, pp. 477–491, 1988.

[27] Z. Ercan, A. Carvalho, S. Lefèvre, H. E. Tseng, M. Gokasan, and F. Borrelli, *Torque-Based Steering Assistance for Collision Avoidance During Lane Changes*. Boca Raton, FL, USA: CRC Press, 2016, pp. 43–48.

[28] P. Gill, W. Murray, M. Saunders, and M. Wright, "User's guide for NPSOL," Syst. Optim. Lab., Stanford Univ., Stanford, CA, USA, Tech. Rep. SOL-86-2, 1986.

**Ziya Ercan** received the B.Sc. degree in electrical and electronics engineering from Anadolu University, Eskisehir, Turkey, in 2008 and the M.Sc. degree in 2011 in control and automation engineering from Istanbul Technical University, Istanbul, Turkey, where he is currently working toward the Ph.D. degree in control and automation engineering.

He is currently conducting a research at the Model Predictive Control Laboratory, University of California, Berkeley, Berkeley, CA, USA, on control algorithms for shared automated driving applications. His research interests include model predictive control, state and parameter estimation, optimization, and machine learning.

**Ashwin Carvalho** received the B.Tech. degree in mechanical engineering from the Indian Institute of Technology, Bombay, Mumbai, India, in 2011. He is currently working toward the Ph.D. degree in mechanical engineering at the University of California (UC), Berkeley, Berkeley, CA, USA, with minors in artificial intelligence and optimization.

He is currently with the Model Predictive Control Laboratory at UC Berkeley working on control strategies for the safe operation of autonomous passenger vehicles in uncertain and dynamic environments. His research interests include stochastic model predictive control, environment modeling, and real-time optimization for control under uncertainty.

**Metin Gokasan** received the B.Sc., M.Sc., and Ph.D. degrees from Istanbul Technical University, Istanbul, Turkey, all in electrical and control engineering, in 1980, 1982, and 1990, respectively.

He is currently a Professor in the Electrical and Electronics Engineering Faculty and the Director of the Mechatronics Engineering Research and Application Center at Istanbul Technical University. Between 2003 and 2006, he conducted his research at the University of Alaska, Fairbanks, AK, USA, as a visiting scholar, where he worked on several projects involving the control of HEVs and sensorless control of induction motors. His research interests include control of electrical machinery, power electronics and electrical drives, control of hybrid electric vehicles, and mechatronics systems.

**Francesco Borrelli** received the "Laurea" degree in computer science engineering from the University of Naples "Federico II," Naples, Italy. He received the Ph.D. from the Automatic Control Laboratory, ETH-Zurich, Zurich, Switzerland, in 2002.

He is currently a Professor in the Department of Mechanical Engineering, University of California, Berkeley, Berkeley, CA, USA. He is the author of more than 100 publications in the field of predictive control and the book *Constrained Optimal Control of Linear and Hybrid Systems* (Springer-Verlag). His research interests include constrained optimal control, model predictive control and its application to advanced automotive control, and energy efficient building operation.

Prof. Borrelli received the 2009 NSF CAREER Award and the 2012 IEEE Control System Technology Award. In 2008, he was the Chair of the IEEE Technical Committee on Automotive Control.